Transmission grating filtering and polarization characteristics in EUV

Mike Gruntman

Department of Aerospace Engineering, MC-1191
University of Southern California, Los Angeles, California 90089-1191

ABSTRACT

Free-standing transmission gratings will be used in a new generation of space instruments for magnetosphere energetic neutral atom (ENA) imaging which requires efficient suppression of the exceptionally strong background extreme ultraviolet (EUV) and UV radiation. The first results of the experimental study of grating (period 200 nm) optical properties in the 50-130 nm wavelength range are presented. It is shown that grating transmission strongly depends on polarization of the incident radiation which makes gratings efficient polarizers. Possibilities of using a single grating and crossed gratings for EUV filtering are discussed.
Keywords: transmission gratings; polarization; EUV; EUV filters; diffraction filters

1. INTRODUCTION

Filtering the radiation in the extreme ultraviolet (EUV) spectral range is required in many space and laboratory applications. Imaging of the heliosphere and planetary magnetospheres in fluxes of energetic neutral atoms (ENA) is recognized to be a powerful tool in the study of global processes in space.[1-3] ENA detection in space is notoriously difficult[1,4] because of extremely low intensity of neutral atom fluxes and because of ENA instrument exposure to a high level of the background EUV/UV radiation (λ<150 nm). The brightness of the background EUV/UV radiation varies from 300 R to 10 kR (1 R = 1 Rayleigh = $10^6/4\pi$ photon cm^{-2} s^{-1} sr^{-1}) depending on experimental conditions. ENA instruments, under gradual development for last 25 years, are rapidly maturing in preparation for the forthcoming space missions, such as Cassini and Magnetosphere Imager.

Currently available techniques to suppress the background EUV/UV radiation limit ENA instrument capabilities and distort ENA characteristics.[1,4] As was first suggested more than a decade ago,[5] diffraction filters can provide efficient suppression of the EUV radiation and high transparency to ENAs. Diffraction filtering is based on the fact that photons can easily pass through a straight channel-pore (slit) in a filter if the channel diameter (slit width) is much larger than the photon wavelength. In contrast to photons, an ENA would pass through the channel freely if it does not collide with channel walls. Thus diffraction filters will allow separation of incident ENAs from EUV/UV photons and would serve as particle collimators.[6] The requirements to filters (to be used in space experiments) include efficient suppression of EUV/UV radiation, high transparency to ENAs (i.e. high geometrical transparency), and mechanical robustness to withstand vibrations and shocks of rocket launch.

Radiation suppression in the EUV/UV spectral range requires diffraction filters with the opening size 100 nm or less. Early work to evaluate submicron structures with the desired properties was started by Gruntman and Leonas[5] for ENA imaging and, simultaneously and independently, by Mitrofanov[7] for EUV astronomical applications. This early work was based on the so called nuclear track filters (see review[6]). Technology of nuclear track filter (NTF) fabrication as well as NTF various applications are described in detail elsewhere.[8-10] Although the EUV/UV filtering by NTFs was successfully demonstrated,[7,11] NTFs are of limited practical use for ENA imaging because of their inherently low geometrical transparency.[6] The review (at 1991 SPIE Meeting[6]) of several possible alternative technologies pointed to promising characteristics of free-standing transmission gratings that should both attenuate and polarize radiation.

Data on EUV radiation transmission through submicron openings are scarce.[12-14] Our experimental study of filtering and polarization properties of free-standing transmission gratings is presented here for the 52–131 nm wavelength range. Some results of this work are discussed elsewhere.[14] A filter based on free-standing transmission gratings would make it possible to separate (transmit) charged and neutral particles from the background EUV/UV radiation (which would be suppressed). Unique properties of such filters will allow substantial improvement in performance of instruments for detection of energetic neutral atom (ENA) fluxes in space plasmas.[6] Diffraction filters can be used for suppression of the background EUV/UV radiation in fusion plasma diagnostics as well.

2. FREE-STANDING TRANSMISSION GRATINGS

The schematic view of a free-standing transmission grating is shown in Fig.1. The grating consists of a set of parallel gold bars with the period, p , and the geometrical transparency, g = d/p, approximately one half. The grating bars are supported by an additional large-mesh grid (not shown in the figure) that makes an overall grating geometrical transparency ≈ 0.25. Gratings are manufactured at the Massachusetts Institute of Technology by a sequence of technological steps including holographic lithography, ion and reactive-ion etching, and electroplating.[15,16] The gratings are being developed for NASA's Advanced X-Ray Astrophysics Facility (AXAF) where several hundred transmission gratings will be flown as a part of the HETG instrument. Though the AXAF requirements are confined to thin film-supported gratings, a spin-off of the new technology is free-standing transmission gratings. Free-standing transmission gratings are designed to withstand mechanical requirements of space flight and will be flown first time on the SOHO mission.[12]

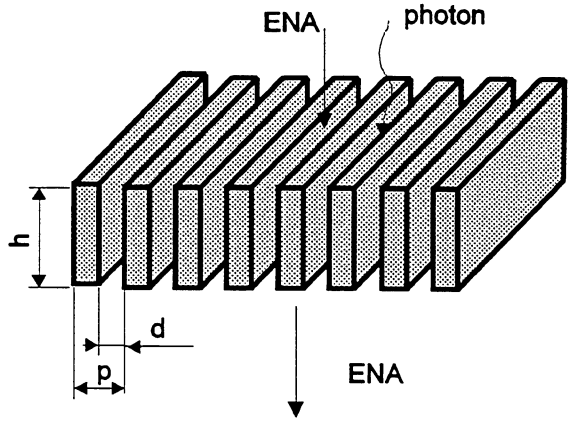

Fig.1. Schematic view of a free-standing transmission grating

We studied one type of the gratings with the following nominal geometrical characteristics (as provided by the manufacturer): period p = 200 nm, distance between the metal bars d = 100 nm (i.e. geometrical transparency g = 0.5), and length h = 435 nm (Fig.1); the grating area is 5×11 mm. The grating would serve as a ±6.6° particle collimator in one dimension. Geometrical transparency of a large-mesh grid supporting the grating is 0.48. This type of gold gratings is commercially available from X-Opt Inc., Gainesville, FL 32605. Characterization of fabricated transmission gratings is a non-trivial task, and geometrical characteristics of gratings may differ from the nominal characteristics.[13,14]

3. EXPERIMENT

Grating filtering and polarization properties are interdependent since the grating transmission strongly depends on the incident light polarization. This polarization dependence significantly complicates experimental study of grating properties which requires accurate knowledge of the photon beam polarization. The method of deriving grating optical characteristics is discussed below in the Section 4. The schematic of the experiment is shown in Fig.2. Monochromatic EUV radiation was produced by a DC glow discharge source followed by a 0.5-m Seya-Namioka EUV monochromator. The collimated photon beam entered the vacuum chamber where the measurements were performed. The layout of the experimental setup is shown in Fig.3.

The light produced by a glow-discharge source is unpolarized, but it becomes partially polarized after reflecting from the diffraction (reflection) grating in the Seya-Namioka monochromator. A gold diffraction (reflection) grating with 1200 line/mm and blazed at 70 nm was used in the monochromator. The polarization of the light exiting the monochromator (which is used to study transmission gratings) is unknown. It is assumed that the light beam consists of two linearly polarized components (along mutually perpendicular X and Y axes) with intensities I_X and I_Y; the total photon beam intensity is $I_0 = I_X + I_Y$ (Fig.2). The X axis is parallel to the grooves of the diffraction grating in the monochromator (i.e. normal to the plane of incidence)

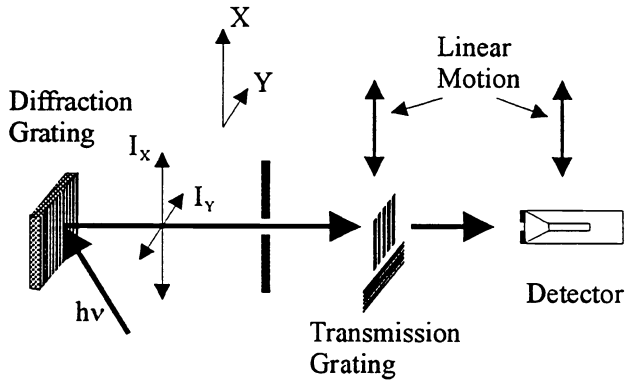

Fig.2. Schematic of the experiment to measure grating transmission and polarization characteristics.

and the Y axis is parallel to the incidence plane; the X and Y axes are perpendicular to the photon beam direction. Polarization, P_0, of the light exiting the monochromator is given by

$$P_0 = (I_X - I_Y)/(I_X + I_Y) \qquad (1)$$

A transmission grating, mounted normal to the photon beam, can be moved in and out of the beam by a linear motion mechanism (Fig.2). A photon detector (channel electron multiplier) can be also moved in the direction perpendicular to the beam axis. Alignment of both the grating and the detector in the Y-axis direction was achieved by additional rotary motion. This experimental arrangement allowed us to measure transmission of the transmission gratings as well as to monitor the background count rate. It was verified by detector scanning that the zero-th diffraction order beam was always measured after the grating. The photon beam was collimated by several slits (Fig.2 and 3), and the detector aperture was selected in such a way as to intercept all transmitted photons in the 0-th diffraction order. The channel electron amplifier was in a linear counting mode; no attempt to account for (possible small) detection efficiency dependence on light polarization[17] has been made. Twelve reliably identified spectral lines were used for transmission measurements in the range from 52.2 through 130.4 nm; helium was used as a working gas in the DC glow discharge light source.

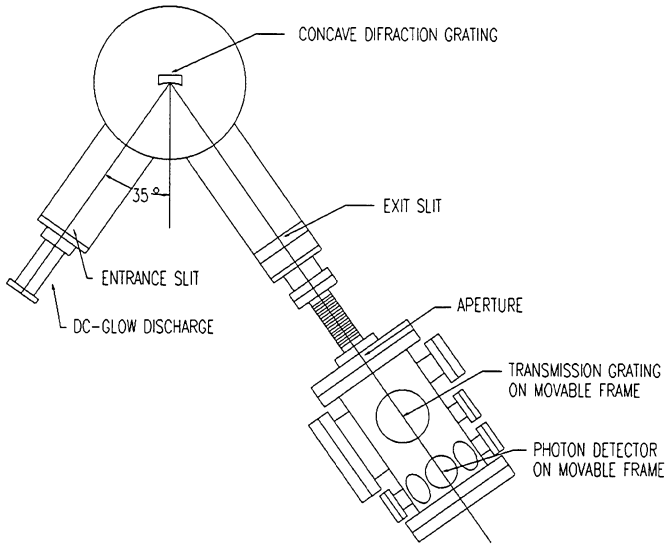

Fig.3 Layout of the experimental setup to study filtering and polarization properties of transmission gratings.

The following measurements were performed:
1) Measurements of single grating transmission for two orthogonal grating orientations: one with the grating metal bars parallel to the reflection grating in the monochromator (i.e. parallel to the X-axis), and another for the perpendicular orientation (i.e. parallel to the Y-axis).
2) Measurements of the transmission of two "crossed" gratings (i.e. two gratings normal to the beam and installed in series, or tandem, with perpendicularly oriented metal bars).

4. MODEL

Let the grating transmission, T_P, be the transmission of the light polarized parallel to the transmission grating metal bars, and the grating transmission, T_S, be the transmission of the light polarized perpendicular to the grating metal bars. It is assumed that the incident light beam, which is linearly polarized parallel (perpendicular) to the grating bars, is attenuated without production a component perpendicular (parallel) to the grating bars after the grating.

The following intensities (detector count rates) are measured: intensity of the unobstructed photon beam (count rate, C_0) and intensity of the attenuated beam (at the 0-th diffraction order) with two grating orientations, *viz.* grating bars parallel to the X-axis (count rate, C_X) and Y-axis (C_Y), respectively. It is convenient to present measurement results using normalized counts rates, $R_X = C_X/C_0$ and $R_Y = C_Y/C_0$, which allows one to eliminate the unknown photon detection efficiency of the detector. The normalized count rates can be related to the grating transmissions, $T_P(\lambda)$ and $T_S(\lambda)$, as

$$R_X(\lambda) = [I_X(\lambda)\, T_P(\lambda) + I_Y(\lambda)\, T_S(\lambda)] / I_0(\lambda) \qquad (2)$$

and

$$R_Y(\lambda) = [I_X(\lambda)\, T_S(\lambda) + I_Y(\lambda)\, T_P(\lambda)] / I_0(\lambda) \qquad (3)$$

By adding and subtracting (2) and (3), one obtains the sum, T_Σ, of single grating transmissions

$$T_\Sigma(\lambda) = T_P(\lambda) + T_S(\lambda) = R_X(\lambda) + R_Y(\lambda) \qquad (4)$$

and the polarization of the incident light, P_0, i.e. the light exiting the monochromator

$$P_0(\lambda) = (R_X(\lambda) - R_Y(\lambda)) / (T_P(\lambda) - T_S(\lambda)) \qquad (5)$$

The transmission, T_X, of the crossed grating configuration would be

$$T_X = T_P \times T_S \qquad (6)$$

and it is independent of the incident light polarization. Thus by experimentally determining the sum of single grating transmissions, T_Σ, (by measuring R_X and R_Y) and measuring the transmission, T_X, of crossed gratings, one unambiguously obtains the grating transmissions, T_P and T_S. The knowledge of the transmissions, $T_P(\lambda)$ and $T_S(\lambda)$, will allow determination of radiation filtering (suppression) properties of various grating configurations.

The filtering of unpolarized light by a single transmission grating is an important for applications case. A single transmission grating would attenuate the light and serve as a polarizer. The transmission of the incident unpolarized light, T_0, by a single grating would be

$$T_0 = (T_P + T_S)/2 = T_\Sigma/2 \qquad (7)$$

and the polarization, P_T, of the transmitted light would be

$$P_T = (T_P - T_S)/(T_P + T_S) \qquad (8)$$

The transmitted light would be highly polarized if $T_P >> T_S$ (i.e. the ratio of transmissions, $T_R = T_P/T_S >>1$); in such a case a transmission grating would serve as an efficient polarizer. The suppression of unpolarized light by a single grating depends on the transmission $(T_P + T_S) = T_\Sigma$ only, and the determination of T_Σ does not require measurements with the crossed gratings.

If one assumes that the ratio of transmissions, T_R, is very large (see Sections 5 and 6), then the polarization of the light produced by the monochromator (equation 5) can be related to measured values, R_X and R_Y, in the following way

$$P_0(\lambda) = (R_X(\lambda) - R_Y(\lambda)) / (T_P(\lambda) - T_S(\lambda)) \approx (R_X(\lambda) - R_Y(\lambda)) / (R_X(\lambda) + R_Y(\lambda)) \qquad (9)$$

The light polarization (produced by our Seya-Namioka monochromator) determined according the equation (9), is the highest at 58.4 nm (P_0=0.8) and, with the wavelength increase, the polarization decreases down to P_0=0.2 at 121.6 nm.

5. THEORETICAL DESCRIPTION

An adequate theoretical model of the radiation transmission through gratings is highly desirable to predict grating filtering properties without expensive try-and-error fabrication. The only known to the author comprehensive theoretical model and the computer code simulating transmission grating optical properties were developed by Erik Anderson.[18] The discussion of the model and computer code can be found elsewhere.[13,18]

The complex dielectric constants, $\varepsilon = \varepsilon_1 - i\varepsilon_1$, of the grating material (gold), are used as input parameters for the computer code.[18] The dielectric constants are related to the index of refraction, n, and the extinction coefficient, k, through the following equations: $\varepsilon_1 = n^2 - k^2$ and $\varepsilon_2 = 2nk$. Optical characteristics of gold in the EUV spectral range are known with some uncertainty,

and they may depend on fabrication specifics and surface preparation technique. We tried in our computer simulations two sets of gold optical constants, those given by Weaver, Krafka, Lynch, and Koch[19] and Lynch and Hunter.[20] These optical constant sets are referred further as the WKLK and LH sets respectively.

Fig.4 shows the spectral dependence of optical constants, n and k, for the WKLK and LH sets. Spectral dependences of ε_1 and ε_2 are shown in Fig.5. The optical constants are given in points where experimental measurements were performed. We also extended computer simulation beyond the experimentally studied spectral range down to 30.4 nm to include this important for space applications line. All points are connected by straight lines to guide the eye.

One can clearly see that two optical constant sets are compatible for short wavelengths, $\lambda<60$ nm, but show a substantial discrepancy for longer wavelengths. Computer simulations performed for both optical constant sets showed that the transmission, T_S, is especially sensitive (up to a factor 40) to the uncertainty in optical constants for $\lambda>80$ nm while the transmission, T_P, varies only slightly (factor 2). Since $T_P >> T_S$ for $\lambda>80$ nm (see below), the transmission, T_Σ, and consequently predictions of the transmission of unpolarized light by a single grating would thus be only slightly sensitive to the uncertainty in optical constants. The difference between the values of T_Σ computed for the LH and WKLK gold constant sets gradually increases with the wavelength increase, and this difference does not exceed a factor of two.

The transmission of unpolarized light by crossed gratings, T_X, which is determined by a product of T_P and T_S, strongly depends on optical constants. The difference between computed values of the transmission, T_X, for two optical constant sets is small at short wavelengths and increases significantly for longer wavelengths.

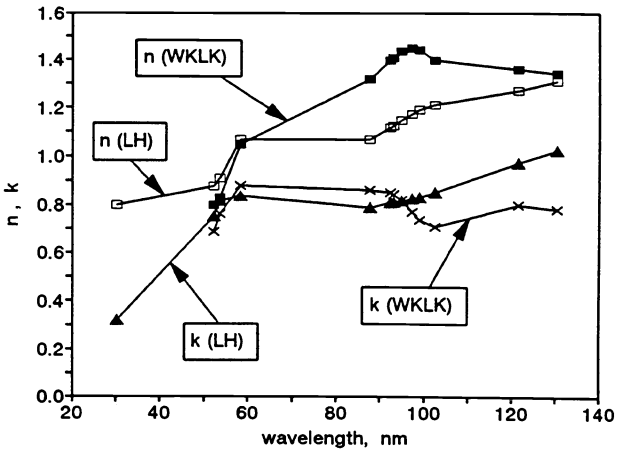

Fig.4. Spectral dependence of the index of refraction, n, and the extinction coefficient, k, for gold; WKLK[19] and LH.[20]

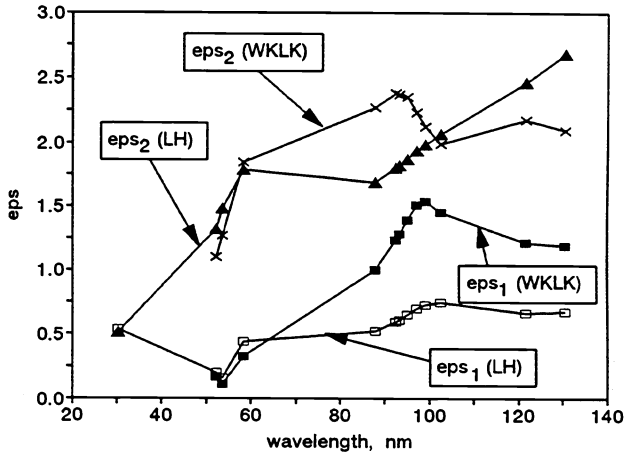

Fig.5. Spectral dependence of the dielectric constants, ε_1 (eps1)and ε_2 (eps_2), for gold; WKLK[19] and LH.[20]

6. EXPERIMENTAL RESULTS AND COMPUTER SIMULATION

The sum of single grating transmissions, $T_\Sigma=T_P+T_S$, was experimentally obtained at 12 wavelengths in the range from 52.2 to 130.4 nm. The transmission, T_X, by crossed gratings was measured at the 58.4 nm wavelength only. The measured dependence $T_\Sigma(\lambda)$ is compared with the computer simulation results in Fig.6; computations are presented here for the LH optical constant set only. The measurement accuracy is better than ± 5 % and it is determined by the counting statistics and experimentally monitored stability of the light beam. Here and further below, all experimental points as well as calculated points are connected by straight lines to guide the eye.

The computed spectral dependence of the grating transmission, which uses nominal grating geometrical parameters (g=0.5), differs substantially from measurement results (Fig.6). Experimentally determined values of $T_\Sigma(\lambda)$ are not only much lower, for

example factor 30 at 121.6 nm, but also the spectral dependence of the transmission is different. With the wavelength decrease all curves are approaching the geometrical transparency of the grating.

The ratio of transmissions, $T_R = T_P/T_S$, is a convenient parameter to describe grating polarization properties. The ratio, T_R, was experimentally determined at the 58.4 nm wavelength (Fig.7), which required measurement of the transmission of two crossed gratings. The measured grating transmission, T_S, is approximately factor 100 smaller than the value of T_P at this wavelength: $T_S = 1.90 \times 10^{-4}$ and $T_P = 1.88 \times 10^{-2}$. The attenuation of unpolarized light (58.4 nm) would be approximately 10^{-2} and 4×10^{-6} by a single grating filter and a crossed gratings filter respectively. The large value of T_R (≈100) demonstrates that transmission gratings would serve as efficient polarizers. For example unpolarized incident radiation at 58.4 nm wavelength will be highly polarized ($P_T \approx 0.98$) after the grating. The experimental value of T_R (Fig.7) is more than a factor 10 higher than the theory prediction for the nominal grating geometrical characteristics.

During final measurements of crossed gratings transmission, the gratings were inadvertently damaged. There is a chance that the measurement of T_X (and the derived value of T_S) is partially affected by this accident. However, the effect seems to be small since post accident measurements did not show significant changes in a single grating transmissions. Nevertheless, the results of crossed gratings measurements should be taken with some caution and their validity will be verified in the future. Measurements of T_Σ are not affected at all.

The discrepancies between the computed grating filtering characteristics and measurement results (Fig.6,7) have suggested a possible deviation of grating geometrical characteristics from those provided by the manufacturer. Measurement of grating geometrical characteristics is a non-trivial task; for example a scanning electron microscope can show the structure of the grating surface but cannot reveal possible slit width variations inside the transmission grating.

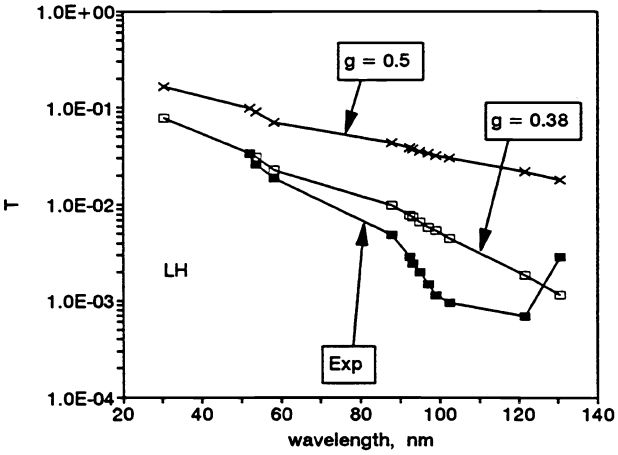

Fig.6. Spectral dependence of the transmission $T_\Sigma = T_P + T_S$. *Exp* curve is the experimentally determined values. Calculated dependences are shown for two different grating geometrical transparencies, g=0.5 and g=0.38.

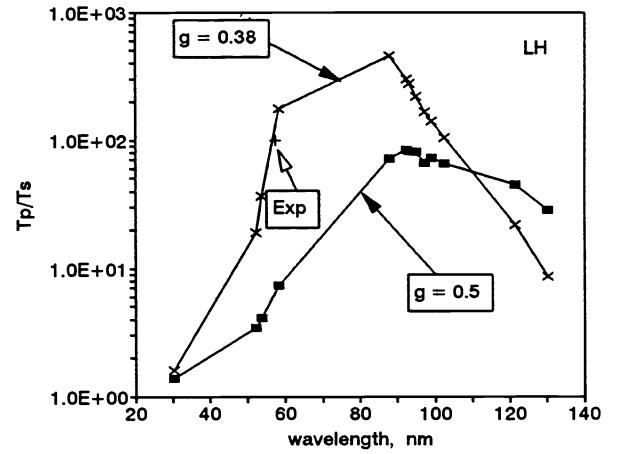

Fig.7. Spectral dependence of the transmission $T_R = T_P/T_S$. *Exp* is the experimentally determined value at 58.4 nm. Calculated dependences are shown for two different grating geometrical transparencies, g=0.5 and g=0.38.

The computed grating transmission is less dependent on the accuracy of theoretical model and uncertainty in gold constants at shorter wavelengths (the transmission approaches the geometrical transparency at very short wavelengths). The grating thickness (455 nm) and period (200 nm) are fixed by the fabrication technology (Mark Schattenburg, private communication); the grating geometrical transparency (or efficient geometrical transparency), g, is more difficult to control and it may vary (i.e. the gap width, d, may vary). Therefore one can assume that the grating period, p, and thickness, h, are known. By varying the geometrical transparency, g, one can try to fit model predictions to the experimentally observed grating transmission, T_Σ, at the shortest wavelength where measurements are available (λ=52.2 nm in our case). The geometrical transparency, g=0.38, provided the best fit. It should be noted that geometrical transparency of another grating that was determined by ion beam attenuation[16] also produced geometrical transparency values smaller than those provided by the manufacturer.

Computer simulations of spectral dependences $T_\Sigma(\lambda)$ and $T_R(\lambda)$ for g=0.5 and g=0.38 are compared in Fig.6 and 7 for the LH gold set. One can see that grating characteristics strongly depend on the parameter, g. The assumption of the smaller geometrical transparency, g=0.38, results in a significantly better agreement between the calculated transmission, $T_\Sigma(\lambda)$, and experimental data, although some differences in the spectral dependence still remain. The agreement of the predicted transmission ratio, T_R, with the experimentally obtained value is excellent (Fig.7) at the 58.4 nm wavelength. Definitive verification of the computer code will require measurements of T_P and T_S at larger number of wavelengths. Large values of the transmission ratio, T_R, requires that even the synchrotron light sources, which provide highly-polarized radiation and look attractive for future grating studies, should be considered as being partially polarized because of the finite angles of acceptance into the monochromator system.[21]

8. LIGHT DIFFRACTION

A transmission grating can serve as a diffracting element in a simple spectrometer. Such a spectrometer was developed to monitor major solar EUV lines and will be flown as a part of the SOHO mission.[12] Figure 8 demonstrates experimentally measured diffraction at 58.4 nm. Computer simulations predict "bright" non-zero diffraction maxima. Calculated radiation intensities for the 1-st, 2-nd, and 3-rd diffraction maxima are shown in Fig.9 for 58.4 nm.. One can see that two sets of gold optical constants give close results. Since diffraction occurs at large angles (up to 90°), a careful design of the detector aperture is required in order to assure interception of diffracted radiation. Our present detector aperture does not allow direct quantitative comparison of the measurements with the theory predictions. Accurate measurement of radiation distribution across diffraction maxima is an important for experimental verification of the computer code[18] and such measurements will be done by us in the future.

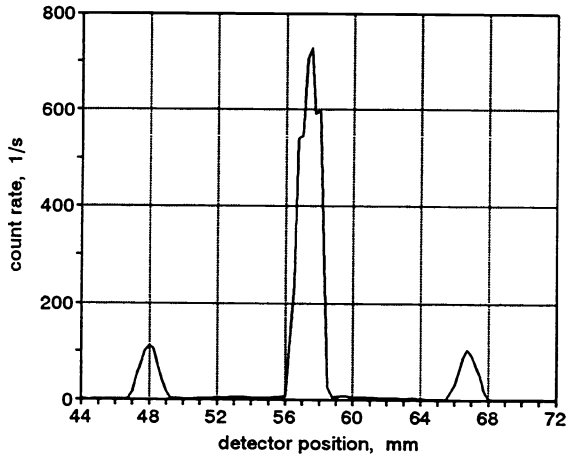

Fig.8. Detector count rate as a function of the distance from the axis (diffraction angle); $\lambda = 58.4$ nm; WKLK[19] and LH.[20]

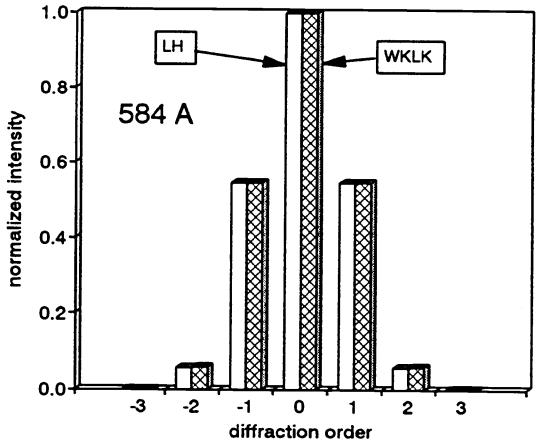

Fig.9. Calculated radiation intensity distributions across diffraction maxima; $\lambda = 58.4$ nm; WKLK[19] and LH.[20]

9. TRANSMISSION GRATINGS AS POLARIZERS AT LONGER WAVELENGTHS

Using the computer code,[18] we simulated polarization properties of transmission gratings at longer wavelengths, in the 200-400 nm spectral range. Since the grating period should be comparable to the radiation wavelength in order to achieve efficient polarization, we performed computer simulation for gratings with the following geometrical characteristics: grating period, p=500 nm; geometrical transparency, g = 0.4; and length, h = 1000 nm. Calculated spectral dependence of the sum of transmissions, $T_\Sigma=T_P+T_S$, and the transmission ratio, $T_R=T_P/T_S$, are shown in fig.10 and 11 respectively. Grating material is gold. One can see that transmission gratings are excellent polarizers in this important for applications UV spectral range. First attempts to maximize grating polarization efficiency (to achieve $T_R = (1\text{-}10)\times10^3$) by varying grating geometrical

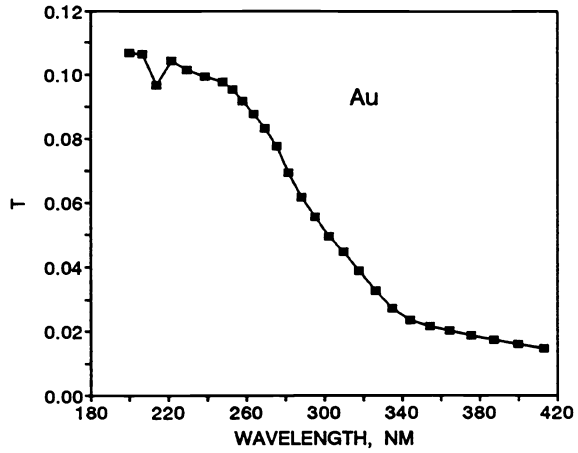

Fig.10. Calculated spectral dependence of the transmission, $T_\Sigma=T_P+T_S$. Grating material is gold; grating period, p=500 nm; geometrical transparency, g=0.4; and length, h=1000 nm

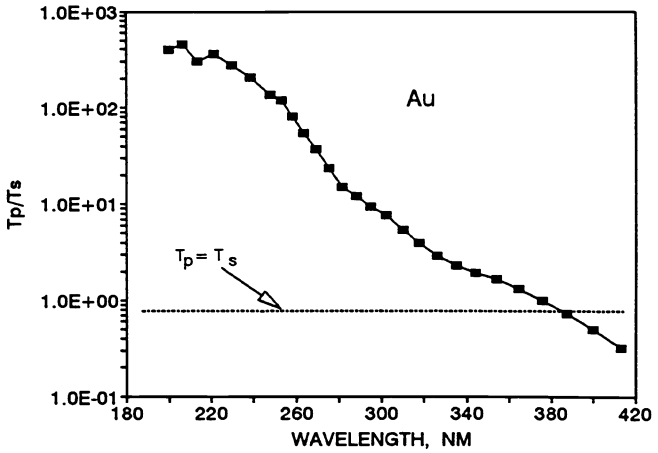

Fig.9. Calculated spectral dependence of the ratio of transmissions, $T_R=T_P/T_S$. Grating material is gold; grating period, p=500 nm; geometrical transparency, g=0.4; and length, h=1000 nm

parameters did not succeed because computational instabilities developed during the program execution. The cause of the code computational instabilities are not understood yet and are being presently investigated.

10. CONCLUSION

The presented experimental study and computer simulations show that transmission gratings serve as efficient filters and polarizers in the EUV/UV spectral range. Depending on applications, filters based on transmission gratings can use both crossed gratings configurations and standing alone single gratings. A crossed grating filter would limit the field-of-view of ENA instrument. ENA cameras with a wide field-of-view in one dimension can be built on the basis of single transmission grating filters. Application of transmission grating-based filters will significantly improve performance of space instruments for planetary magnetosphere and heliosphere ENA imaging and will provide enhanced capabilities for various EUV/UV instruments.

11. ACKNOWLEDGMENT

The work is supported by the NASA Grant NAGW-3520. Erik Anderson, Darrell Judge, Don McMullin, Howard Ogawa, Lev Pitaevskii, Mark Schattenburg, and Earl Scime showed interest and provided kind help during this work. It is my pleasure to acknowledge their support.

12. REFERENCES

1. K.C. Hsieh, C.C. Curtis, C.Y. Fan, and M.A. Gruntman, "Techniques for remote sensing of space plasma in the heliosphere via energetic neutral atoms: a review," in *Solar Wind Seven*, eds. E. Marsch and R. Schwenn, 357-364, Pergamon, New York, 1991.

2. D.J. Williams, E.C. Roelof, and D.G. Mitchell, "Global magnetosphere imaging," *Rev. Geophys.*, v.30, 183-208, 1992.

3. M.A. Gruntman, "Anisotropy of the energetic neutral atom flux in the heliosphere," *Planet. Space Sci.*, v.40, 439-445, 1992.

4. R.W. McEntire and D.G. Mitchell, "Instrumentation for global magnetosphere imaging via energetic neutral atoms," in *Solar System Plasma Physics*, eds. J.H. Waite Jr., J.L. Burch, and R.L. Moore, 69-80, AGU, Washington, DC, 1989.

5. M.A.Gruntman and V.B. Leonas, "Neutral solar wind: possibilities of experimental investigation," *Report (Preprint)* 825, Space Research Institute (IKI), Academy of Sciences, Moscow, 1983.

6. M.A. Gruntman, "Submicron structures: promising filters in EUV - a review," *EUV, X-Ray, and Gamma-Ray Instrumentation for Astronomy*, eds. O.H. Siegmund and R.E. Rothschield, *Proc. SPIE* 1549, 385-394 , 1991.

7. A.V. Mitrofanov, "Structurally nonuniform filters for the vacuum ultraviolet and ultrasoft X-ray regions of the spectrum," *Instrum. Exp. Techn.*, v.26(4), 971-974, 1983.

8. G.N. Flerov and V.S. Barashenkov, "Practical applications of heavy ion beams," *Sov. Phys. - Usp.*, v.17(5), 783-793, 1975.

9. B.E. Fischer and R. Spohr, "Production and use of nuclear tracks: imprinting structure on solids," *Rev. Mod. Phys.*, v.55(4), 907-948, 1983.

10. R. Spohr, *Ion Tracks and Microtechnology*, Friedriech Vieweg & Sons Verlagsgesellschaft mbh, Braunschweig, 1990.

11. A.V. Mitrofanov and P.Yu. Apel, "Porous plastic membranes used as extreme and far ultraviolet radiation diffraction filters," *Nucl. Instrum. Methods Phys. Res. A*, v.282, 542-545, 1989.

12. H.S. Ogawa, D.R. McMullin, D.L. Judge, and R. Korde, "Normal incidence spectrophotometer with high density transmission grating technology and high-efficiency silicon photodiodes for absolute solar extreme-ultraviolet irradiance measurements," *Optical Engin.*, v.32(12), 3121-3125, 1993.

13. E.E. Scime, E.H. Anderson, D.J. McComas, and M.L. Schattenburg, "Extreme ultraviolet polarization and filtering with gold transmission gratings," *Appl. Optics*, v.34(4), 648-654, 1995.

14. M.A. Gruntman, "EUV radiation filtering by free-standing transmission gratings," *Appl. Optics*, in press, 1995.

15. M.L. Schattenburg, E.H. Anderson, and H.I. Smith, "X-ray/VUV transmission gratings for astrophysical and laboratory applications," *Physica Scripta*, v.41, 13-20, 1990.

16. J.M. Carter, D.B. Olster, M.L. Schattenburg, A. Yen, and H.J. Smith, "Large-area, free-standing gratings for atom interferometry produced using holographic lithography," *J. Vac. Sci. Technol. B*, v.10(6), 2909-2911, 1992.

17. J. Tomc, P. Zetner, W.R. Westerveld, and J.W. McConckey, "Variations in the polarization sensitivity of microchannel plates with photon incidence angle and wavelength in the VUV," *Appl. Optics*, v.23(5), 656-657, 1984.

18. E.H. Anderson, "Fabrication and electromagnetic applications of periodic nanostructures," *Ph.D. Thesis*, Massachusetts Institute of Technology, 1988.

19. J.H. Weaver, C. Krafka, D.W. Lynch, and E.E. Koch, *Optical Properties of Metals*, Pt.2, Nr.18-2, Fachinformationszentrum Energie, Physik, Mathematik GMbH, Karlsruhe, 1981.

20. D.W. Lynch and W.R. Hunter, in *Handbook of Optical Constants of Solids*, ed. E.D. Palik, Academic Press, p.275-295, 1985.

21. J.A.R. Samson, "Polarized vacuum ultraviolet and X-radiation," *Nucl. Instrum. Meth.*, v.152, 225-230, 1978.